



Computer Science and Artificial Intelligence Laboratory
Technical Report

MIT-CSAIL-TR-2015-032

November 24, 2015

**Representation Discovery for
Kernel-Based Reinforcement Learning**
Dawit H. Zewdie and George Konidaris

Representation Discovery for Kernel-Based Reinforcement Learning

Dawit H. Zewdie
Learning and Intelligent Systems Group
MIT, CSAIL
Cambridge, MA 02139
dawit@alum.mit.edu

George Konidaris
Intelligent Robot Lab
Duke University
Durham, NC 27708
gdk@cs.duke.edu

Abstract

Recent years have seen increased interest in non-parametric reinforcement learning. There are now practical kernel-based algorithms for approximating value functions; however, kernel regression requires that the underlying function being approximated be smooth on its domain. Few problems of interest satisfy this requirement in their natural representation. In this paper we define **value-consistent pseudometric (VCPM)**, the distance function corresponding to a transformation of the domain into a space where the target function is maximally smooth and thus well-approximated by kernel regression. We then present **DKBRL**, an iterative batch RL algorithm interleaving steps of Kernel-Based Reinforcement Learning and distance metric adjustment. We evaluate its performance on Acrobot and PinBall, continuous-space reinforcement learning domains with discontinuous value functions.

1 Introduction

Kernel-based reinforcement learning (KBRL) methods have recently begun to receive significant research attention [1, 2, 3, 4, 5]. These algorithms have the virtue of being non-parametric: their computational complexity scales with the amount of data, rather than with the size of the state space; consequently, they are a promising means of avoiding the so-called *curse of dimensionality*, where the number of parameters in a parametric representation of a general value function scales exponentially with the dimensionality of the state space.

Key to these algorithms is the use of kernel regression to extrapolate values. Kernel regression is a smooth-function approximation technique that performs all computation in terms of distance in the state space.

Kernel regression has difficulty modelling discontinuous functions. This difficulty can be alleviated by adding more data, but doing so is often undesirable. We show that changing the distance metric used in the regression can efficiently resolve the difficulties. Existing metric learning algorithms are not, in general, capable of dealing with discontinuities. We introduce the notion of a *value-consistent pseudometric (VCP)* and show that it allows kernel-regression to model discontinuous functions. We then present a novel iterative algorithm for approximating the VCP, and evaluate its performance on Acrobot and PinBall, two reinforcement learning domains with discontinuous value functions.

2 Background

Reinforcement learning [6] problems are typically formalized as Markov Decision Processes (MDPs) [7], which can be described by a tuple $\langle S, A, T, R, \gamma \rangle$, where S is a possibly infinite set

of states, A is a finite set of actions, $T : S \times A \times S \rightarrow [0, 1]$ is an expression of the probability that a given action will result in a particular state transition $R : S \times A \times S \rightarrow \mathbb{R}$ is an expression of the reward received for each possible state transition, and γ is a discount factor specifying how much the agent prefers immediate rewards to future ones. The agent starts the process in some start state, s_0 , and chooses an action a_t based on s_t at every time step t , causing the state to change to state s_{t+1} with probability $T(s_t, a_t, s_{t+1})$, and the agent to receive reward $r_t = R(s_t, a_t, s_{t+1})$. The reward and transition functions are assumed to be unknown; the agent must learn how to act by observing sample rewards and transitions. In this paper, we assume that the agent is given a batch of sample transitions from which to learn.

The agent picks actions by a policy $\pi : S \rightarrow A$. The total reward the agent can expect when following π starting from state s is denoted $V^\pi(s) = E[\sum_i \gamma^i r_i | s_0 = s, a_i = \pi(s_i)]$. The agent’s objective is to maximize this *return*, by finding a policy, π^* , such that $V^{\pi^*}(s) = \max_\pi V^\pi(s)$ for all states s . It is convenient to think in terms of the value of a state-action pair, $Q^\pi(s, a)$, the expected return when taking action, a , in state, s , then following π forever after. $V^\pi(s) = \max_a Q^\pi(s, a)$

When the set of states is small and finite, an MDP can be efficiently solved by value iteration, which uses dynamic programming to find V and Q satisfying

$$Q(s, a) = \sum_{s' \in S} T(s, a, s') [R(s, a, s') + \gamma V(s')].$$

Solving MDPs with continuous state spaces is less straightforward. Popular techniques include LSTD [8], and Sarsa [9] which try to approximate the value function parametrically. With the right parametric form, these algorithms can produce high quality solutions from very little data; however, no amount of data can help them produce a good solutions when they assume the wrong form.

By contrast, non-parametric methods represent the value function directly in terms of the data. This avoids the need for assumptions about value function form and allows the complexity of the fit generated to scale naturally with the amount of data. We are interested in improving KBRL, one particular non-parametric algorithm.

2.1 Kernel-Based Reinforcement Learning

KBRL [1] is a non-parametric value function approximation algorithm for continuous MDPs. It is a three-step process that solves the MDP using a set of sample transitions. The first step constructs a finite approximation of the MDP from the samples, the second step solves that finite approximation, and the third step interpolates that solution to the original state space.

KBRL takes as input a set of sample transitions, $S^a = \{w_i^a = (s_i^a, r_i^a, \hat{s}_i^a) \mid i = 1, \dots, n_a\}$, resulting from each action, a . From these transitions, KBRL constructs a finite MDP, $M' = \langle S', A, T', R', \gamma \rangle$. The new state space, S' , is the set of sample transitions, so $|S'| = n = \sum_a n_a$. The new reward function is $R'(w_i^a, a', w_j^{a'}) = r_j^{a'}$. The new transition function T' is defined as

$$T'(w_i^a, a', w_j^{a'}) = \begin{cases} 0 & \text{if } a' \neq a'' \\ \kappa_{a'}(\hat{s}_i^a, s_j^{a''}) & \text{otherwise,} \end{cases}$$

where $\kappa_a(\cdot, \cdot)$ is some similarity function constrained to be nonnegative, decreasing in the distance between its two arguments, and satisfying $\sum_i \kappa_a(s, s_i^a) = 1$ for all $s \in S$. It is convenient to think of κ as being the normalized version of some underlying *mother kernel*, k , so that $\kappa_a(s, s_i^a) = \frac{k(b^{-1}d(s, s_i^a))}{\sum_j k(b^{-1}d(s, s_j^a))}$ where d is a metric and b is a bandwidth. There is a bias-variance trade-off to be made when choosing b ; bias decreases with b while variance increases [1]. Except where stated otherwise, we use a Gaussian as our mother kernel throughout this paper.

There is work [2] exploring the possibilities for similarity functions (trees, nearest neighbours, and grid-based approximations), but all of it uses Euclidean distance, d_{Euc} , as the metric. The justification is that the value function is assumed smooth—that nearby points have similar values. When it uses d_{Euc} , KBRL can be seen as using local averaging to approximate the transition, reward, and Q-value functions. In the next section we show what happens when the smoothness assumption is not met.

KBRL solves for V' , the value function of M' using some finite MDP solver then generalizes it to M using the equation

$$Q(s, a) = \sum_{w_i^a \in S^a} \kappa_a(s, s_i^a) [r_i^a + \gamma V'(w_i^a)].$$

Note that the size of the finite model, M' constructed by KBRL is equal to the number of sample transitions. This makes solving it computationally intensive, even when using a sparse kernel; however, an approximate solution to M' can be found efficiently if its transition probability matrix is replaced by a low-rank approximation [5]. Kernel-based stochastic factorization (KBSF) takes advantage of this property, using a stochastic factorization of the matrix as the low-rank approximation. KBSF takes time linear in the amount of data and a constant amount of space that depends only on the desired approximation coarseness. Though we only provide proofs and results for KBRL, the ideas presented in this paper can also be applied to KBSF.

3 Importance of the Right Metric

Because of its smoothness assumptions, KBRL is not well suited for solving MDPs whose value functions have cliffs. To see why, consider *TWO-ROOM*, a simple MDP presented in Figure 1. It describes a world with two rooms connected by doorway. The agent can freely move through the open space of the world but cannot go through the wall.¹ A region in one room is marked as the goal. The agent receives a reward of 0 when inside the goal and -1 otherwise.

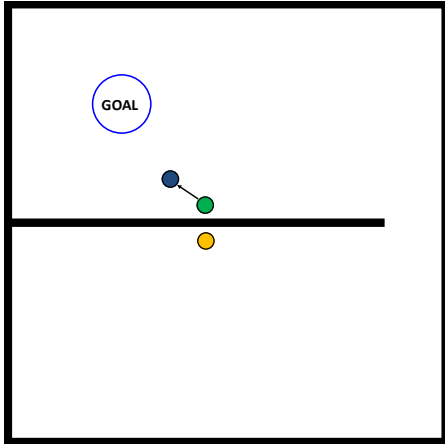


Figure 1: The state space of *TWO-ROOM*. There is a sample transition in the top room and state near the sample in the bottom room

The optimal policy in *TWO-ROOM* is to navigate directly to the goal. Thus, the value of a state, s , is decreasing in the length of the shortest path from it to the goal, $d_{\text{TR}}(s, g)$ (where d_{TR} denotes shortest-path metric). States that are physically close together but on opposite sides of the wall have starkly different values. To solve *TWO-ROOM*, one must faithfully represent this steep drop in value across the wall.

For KBRL to represent the value cliff, it must be run with a small bandwidth. Compensating for the resulting variance requires a large set of sample transitions, making the domain challenging for KBRL. However, if we use d_{TR} instead of d_{Euc} as the metric in the mother kernel, *TWO-ROOM* becomes easily solvable with a large bandwidth and small data set. Since the value function is smooth with respect to d_{TR} we can use large bandwidths with no risk of averaging across the wall.

We tried solving *TWO-ROOM* with different combinations of bandwidth and metric, holding the training set fixed 2. When running KBRL with a large bandwidth and the Euclidean metric, the

¹For the purposes of discussion, assume the agent can move in any direction or choose to stay in place (making for an infinite set of actions).

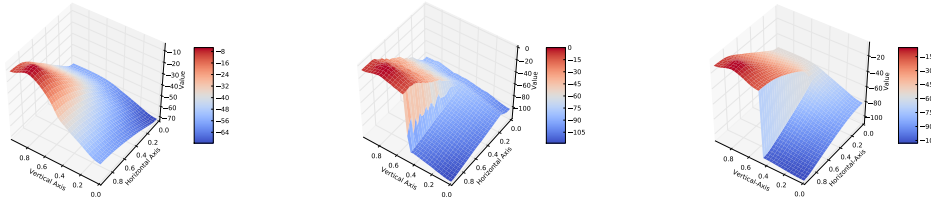


Figure 2: Left to right: *TWO-ROOM*'s value function estimated with d_{Euc} and $b = .06$; with d_{Euc} and $b = .01$; and with d_{TR} and $b = .06$

value cliff is completely smoothed out. The resulting policy has the agent attempt to walk through the wall. With a small bandwidth, KBRL finds the correct overall shape for the value function, but there are some ripples that appear as artefacts of the small bandwidth. The resulting policy has the agent reach the goal on a path that zigzags around the shortest path. Running KBRL with d_{TR} and a large bandwidth produces the correct shape for the value function without any ripples. The resulting policy takes the agent to the goal along the shortest path.

The manifold of the *TWO-ROOM* state space is a square with a line segment cut out of it. The value function is smooth on the manifold but discontinuous in Euclidean space. Thus, using distance on the manifold instead of Euclidean distance makes kernel regression work better. Domains like *TWO-ROOM* have been used to motivate representation discovery in parametric reinforcement learning, most notably by Proto-Value Functions [10] which use the eigenfunctions of the manifold as a basis.

The discontinuity in *TWO-ROOM*'s value function comes from the local connectivity of the state space, but local connectivity is not the only factor that affects value function smoothness. Consider, for instance, a modification to *TWO-ROOM* where the wall is replaced by a region of low reward. The agent can freely move through this region, but would get a better return by going around it. This modification removes the connectivity issues (the state space manifold is Euclidean space) but the value function still has the same discontinuity. Now consider a modification where the agent can jump over the wall if it has enough momentum. With this modification, two states that are close to each other² and far from the wall can have very different values depending on whether the agent is on a trajectory that can hurdle the wall. This modified version of *TWO-ROOM* has a value function discontinuity that extends beyond the wall and no local information can help distinguish the states it separates. Neither d_{Euc} nor d_{TR} do particularly well here.

The cases above show that a good metric must consider more than just local state space topology; it must also account for global dynamics and the reward structure of the MDP. In some sense, knowing the right metric requires already knowing the value function. The next section identifies the ideal metric and provides an algorithm for approximating it.

4 Value-Consistent Pseudometrics

KBRL uses kernel regression to approximate the Q-values of an MDP. It does this using kernels of the form $\kappa_a(s, s') = c_a \cdot k(\frac{d_{Euc}(s, s')}{b})$, where c_a is a normalizing constant. We are interested in finding a new metric d' to replace d_{Euc} in the regression. To keep things simple, we begin by removing the reinforcement learning component of the problem and only considering regression.

²Note that here we are measuring distance in phase space. Two states are nearby if they have similar position and velocity.

4.1 Transforming to Improve Regression

The problem statement of regression is as follows: given a set of training points, $D = \{(x_i, y_i) \mid i = 1, \dots, n\}$, of point-value pairs with $y_i = f(x_i)$ for some $f : X \rightarrow \mathbb{R}$, produce a function \tilde{f} that approximates f well, for some measure of approximation quality.³

Regression with a kernel estimator [11] produces the estimate $\tilde{f}(x) = \frac{\sum_i k(b^{-1}d_{\text{Euc}}(x-x_i))y_i}{\sum_i k(b^{-1}d_{\text{Euc}}(x-x_i))}$. In Section 3, we found that replacing d_{Euc} with a function that varies more closely with f can produce better results. The function that varies most closely with f is the pseudometric⁴ $d_f^*(x, x') = |f(x) - f(x')|$. The diameter of X under d_f^* depends on f . We can remove this dependence using the scalar $\mu_f = \frac{\Delta_X(d_{\text{Euc}})}{f_{\max} - f_{\min}}$ to make $d_f(x, x') = \mu_f d_f^*(x, x')$, a pseudometric with the same diameter as d_{Euc} . d_f is the most natural choice for replacing d_{Euc} in the regression. We call d_f the **value-consistent pseudometric (VCPM)** for f on X .

Unfortunately, to use d_f in the regression one would need to already know f . Our workaround is an iterative algorithm that interleaves steps of regression and metric learning to approximate the VCPM for f on X . We start with an initial metric $d_0 = d_{\text{Euc}}$ and use the kernel estimator to produce an estimate f_1 . We then use f_1 and d_0 to produce a new metric d_1 that corresponds to a representation of X where f_1 is smoother. We then use d_1 in our kernel estimator to get a new estimate f_2 and repeat until the approximation stops improving.

The metric d_i should be a relaxation of d_{i-1} towards d_{f_i} , the VCPM for f_i on X . One way to do this would be to choose $d_i(x, x') = c_0 \sqrt{d_{i-1}(x, x')^2 + \alpha^2 d_{f_i}(x, x')^2}$, where c_0 is a diameter preserving constant and $\alpha > 0$ is a relaxation rate. Note that even though d_{f_i} is a pseudometric, each d_i is guaranteed to be a valid metric on X because of the dependence on d_{i-1} .

The effect of varying α is discussed in the Appendix. The diameter preserving c_0 satisfies $\frac{1}{\sqrt{1+\alpha^2}} \leq c_0 \leq 1$ and is difficult to calculate exactly, so we assume the lower bound. Calculating d_{f_i} requires knowing the extrema of f_i , which are also difficult to compute but known to be bounded by y_{\max} and y_{\min} ; we use these bounds in place of the exact values. With these two heuristics, the metric will underestimate some distances. Underestimating distances is equivalent to using a larger bandwidth, which is an acceptable trade-off for the performance improvement.

With these adjustments, our relaxation of the metric becomes

$$d_i(x, x') = \frac{1}{\sqrt{1 + \alpha^2}} \sqrt{d_{i-1}(x, x')^2 + \left(\alpha \Delta(d_{\text{Euc}}) \frac{f_i(x) - f_i(x')}{y_{\max} - y_{\min}} \right)^2}.$$

This relaxation can be viewed as a transform on X compressing it where f_i is flat and stretching it where f_i is steep. This transform warps the m -dimensional X through $m + i$ dimensions in such a way that f_i becomes smoother. For this reason, we call it a **Dimension-Adding Wrinkle-Ironing Transform (DAWIT)** [12]. Appendix A discusses the geometric interpretation of the transform in more detail.

For reasons explained in Appendix A, we refer to “kernel regression augmented to learn a metric by DAWIT” as FDK. We are able to demonstrate a number of properties of FDK. We have experimental evidence⁵ that the best fit does not always occur in the limit. We also have proof that: in the limit of infinite data and a bandwidth that shrinks at an appropriate rate, the metric learned converges to the VCPM of f on X ; for a fixed bandwidth and dataset, iterating until convergence produces a piecewise flat approximation of f ; the number of pieces in the piecewise flat approximation varies inversely with b .

³We assume that X is a compact, connected subset of \mathbb{R}^m ; and that $\max_i y_i = y_{\max} \neq y_{\min} = \min_i y_i$. From these assumptions it follows that f has distinct extrema on X ; we refer to these as f_{\max} and f_{\min} . We refer to the diameter of X under metric d as $\Delta_X(d)$

⁴ d_f^* is a pseudometric because it doesn't satisfy $d^*(x, x') \implies x = x'$; in the supplementary materials we show that it is safe to use d_f^* as a metric in kernel regression.

⁵see Appendix B

Claim In the limit of infinite data and a bandwidth that shrinks at an admissible rate⁶, performing FDK to convergence with any $\alpha > 0$ will produce the VCPM of the function being approximated.

Proof. (sketch) We show this in two parts: First we show that repeatedly applying DAWIT with the same function produces a sequence of metrics converging to the VCPM for that function on its domain. Next, we use the convergence properties of kernel regression to show that FDK also possesses the property.

Part 1: The metric produced by DAWIT on iteration j satisfies

$$\begin{aligned} d_j(x_1, x_2) &= \sqrt{\frac{d_{j-1}(x_1, x_2)^2 + \alpha^2 \mu_f^2 \cdot (f(x_1) - f(x_2))^2}{1 + \alpha^2}} \\ &= \sqrt{\frac{d_0(x_1, x_2)^2}{(1 + \alpha^2)^j} + \alpha^2 \mu_f^2 \cdot (f(x_1) - f(x_2))^2 \sum_{i=1}^j \frac{1}{(1 + \alpha^2)^i}}. \end{aligned}$$

As $j \rightarrow \infty$, the term involving d_0 goes to zero exponentially quickly and the summation on the right converges to α^{-2} . It follows that

$$\lim_{j \rightarrow \infty} d_j(x_1, x_2) = \mu_f \cdot (f(x_1) - f(x_2))$$

which is the VCPM for f on X .

Part 2: As the size of the dataset increases and the bandwidth decreases at an admissible rate, the first estimate, f_0 , produced by kernel regression converges to f . It follows that the metric d_1 produced by DAWIT converges to a relaxation towards d_f and subsequent iterations of FDK resemble DAWIT repeated with the same function which, as we showed above, converges to the VCPM for the function on its domain. \square

The proof above shows that in the limit, FDK produces the pseudometric we identified as the ideal. Next we show the convergence properties of FDK by characterizing the fixed points of FDK. A pseudometric d is a **fixed point** of FDK on dataset D if performing a round of DAWIT with $d_{i-1} = d$ (and \tilde{f}_i being the result of kernel regression with d_{i-1}) produces $d_i = d$.

Lemma A pseudometric d is a fixed point of FDK if and only if the function \tilde{f} created by performing kernel regression using d satisfies $d(x_i, x_j) = \mu_{\tilde{f}} |\tilde{f}(x_i) - \tilde{f}(x_j)|$ for all $x_i, x_j \in D$.

The proof of this lemma is some straightforward arithmetic substituting into the equation for DAWIT; it is omitted in the interest of space. Next, we say a metric d is an **attractive fixed point** of FDK if there exists $\epsilon > 0$ such that starting FDK from any pseudometric d_0 satisfying $|d_0(x, x') - d(x, x')| < \epsilon$ for all $x, x' \in X$, produces a sequence of converging to d . The set of attractive fixed points is the set of pseudometrics to which FDK can converge.

Claim For a metric, d to be an attractive fixed point, the function \tilde{f} resulting from doing kernel regression with d must be flat at x_i for every $x_i \in D$.

Proof. (by contradiction) Assume d is an attractive fixed point of FDK for a given dataset D such that \tilde{f} is not flat at some $x_i \in D$. Assume WLOG that $i = 1$. \tilde{f} being non-flat at x_1 means in any neighbourhood of x_1 there is some x such that $\tilde{f}(x) \neq \tilde{f}(x_1)$. Note that this can only happen if $d(x, x_1) \neq 0$.

Given some ϵ , Let x^* be a point such that: $(x^*, f(x^*)) \notin D$; $d(x^*, x_1) < \epsilon$; and $\tilde{f}(x^*) \neq \tilde{f}(x_1)$. Let d' be the pseudometric satisfying $d'(x, x^*) = d(x, x_1)$ for all x and $d'(x, x') = d(x, x')$ for all $x, x' \neq x^*$. The approximation \tilde{f}' that results from using d' in kernel regression is identical to \tilde{f} except at x^* , where $\tilde{f}'(x^*) = \tilde{f}(x_1)$ (since x^* is not in D it has no influence over the regression). It follows that \tilde{f}' satisfies the constraints for d' to be a fixed point. Therefore d does not attract d' and cannot be an attractive fixed point. \square

⁶An admissible shrinkage rate [1] is one where the bandwidth goes to zero but slowly enough (relative to the data increase) to avoid creating an undesirable rise in variance.

An implication of the claim above is that, in the limit, neighborhoods of points in the dataset get collapsed into singularities. The supplementary materials provide intuition about how this happens.

In practice, we find that approximation error typically goes down then up, and the metric that minimizes it is found after just a handful of iterations. We also find that our augmented kernel regression is very well suited for modelling discontinuities like the one in *TWO-ROOM*'s value function. Appendix B provides empirical data about fit quality.

Claim When performed using a kernel, k , with compact support having bandwidth, $b < \frac{\Delta x}{c}$, for some integer, c , FDK has an attractive fixed point with $c + 1$ singularities.

Proof. (by construction) Consider the dataset $D = \{(x_i, y_i) \mid i = 0 \dots c\}$ with $x_i = y_i = i$ produced from a function $f : [0, c] \rightarrow \mathbb{R}$. Let d be the pseudometric such that $d(x_i, x_j) = d_{\text{Euc}}(x_i, x_j)$ for all $i, j \in 0, \dots, c$ and $d(x, x_0) = 0$ for all $x \notin \{x_0, \dots, x_c\}$.

First, we show that $d(x)$ is a fixed point. Let \tilde{f} be the function produced by kernel regression using d as the metric. Solving for \tilde{f} gives $\tilde{f}(x) = \sum_j k(x, x_j) y_j$. Because of the constraints on the bandwidth, $k(x_i, x_j) = 0$ for all $i \neq j$, thus $\tilde{f}(x_i) = y_i = x_i$ for all i and $\tilde{f}(x) = y_0 = x_0$ for all $x \notin \{x_0, \dots, x_c\}$. \tilde{f} is a line though all $c + 1$ points in D . By our lemma, this makes it a fixed point.

To show that $d(x)$ is attractive, we consider a new pseudometric that is a perturbation of d . Let d_0 be a pseudometric such that $|d(x, x') - d_0(x, x')| < \frac{\Delta(x)}{c} - b$ for all pairs of points (x, x') in X . The \tilde{f}_0 that results from kernel regression using d_0 satisfies $\tilde{f}_0(x) = \tilde{f}(x)$ because the perturbations were made small enough that kernels centred on each x_i still do not overlap. During the metric learning step, DAWIT produces the metric $d_1(x, x') \propto \sqrt{d_0(x, x')^2 + \alpha^2 \mu^2 (\tilde{f}(x) - \tilde{f}(x'))^2} = \sqrt{d_0(x, x')^2 + (\alpha \mu d(x, x'))^2}$. Note that d_1 is a relaxation towards d . Since d_1 satisfies the constraints we placed on d_0 , it follows that d_2, d_3, \dots , are also relaxations to d and that the sequence $\{d_i\}$ converges to d , making d an attractive fixed point. \square

The proof above shows that the number of pieces in the piecewise flat approximation generated in the limit of FDK is inversely proportional to the bandwidth used. The proof can be extended to deal with kernels with infinite support.

4.2 Transforming to Improve Reinforcement Learning

Now that we have an extension of kernel regression capable of modelling a wider class of functions, we are ready to apply it to reinforcement learning.

It is tempting to think that $d_{V^{\pi^*}}$, the VCPM for V^{π^*} , is the ideal pseudometric. This is not the case; $d_{V^{\pi^*}}$ corresponds to an abstraction where all states with the same value are mapped to the same abstract state. Such an abstraction discards information about the optimal action. What we need is an abstraction where only states with the same Q-values are mapped to the same abstract state.

We can produce such an abstraction by using the VCPMs for the Q-values.⁷ For each action a we want $\kappa_a(s, s'_i) = \frac{k(b^{-1} d_{Q^a}(s, s'_i))}{\sum_j k(b^{-1} d_{Q^a}(s, s'_j))}$. Note that we are using a different pseudometric in the kernel for each action. Using the VCPMs for the Q-values corresponds to a Q^* -irrelevance abstraction; it satisfies $\Phi(s) = \Phi(s') \implies Q^{\pi^*}(s, a) = Q^{\pi^*}(s', a) \forall a$ since $\|\Phi(s) - \Phi(s')\| = 0 \iff d_{Q^a} Q(s, s') = 0 \forall a \iff Q^{\pi^*}(s, a) = Q^{\pi^*}(s', a) \forall a$. Acting optimally with respect to Q-values in a Q^* -irrelevance abstraction results in optimal behaviour in the ground MDP [13].

Now that we have identified the desired abstraction, we can construct an algorithm to approximate it. As we did for regression, we start from the Euclidean metric and iteratively estimate the Q-values (with KBRL) and update our metrics (with DAWIT). Algorithm 1 describes the process.

In practice we found that it was rarely worth doing more than five iterations of DKBRL. There is one important detail that is worth mentioning; the algorithm reuses the same dataset on each iteration

⁷We use Q^a to refer to the function $Q^a(s) = Q^{\pi^*}(s, a)$.

Algorithm 1 DAWIT-KBRL

```
1: procedure DKBRL( $S', b$ )
2:    $d_0^a \leftarrow d_{\text{Euc}} \forall a$ 
3:    $i \leftarrow 0$ 
4:   repeat
5:      $Q_i \leftarrow \text{KBRL}(S', b, d_i)$ 
6:     for  $a \in A$  do
7:        $d_{i+1}^a \leftarrow \text{DAWIT}(d_i^a, Q_i^a)$ 
8:     end for
9:      $i \leftarrow i + 1$ 
10:  until Policy stops improving.
11:  return  $Q_{i-1}$ 
12: end procedure
```

because the problem formulation is to learn from a batch of sample transitions. Were we free to collect fresh data between iterations, we would want the sampled points to be uniformly distributed with respect to the latest metric. Doing so is necessary for KBRL’s correctness guarantees. Uniform coverage with the learned metric is equivalent to concentrating samples in the regions of state space where the Q-values are steep, which is sensible because that is where the Q-values tend to be poorly approximated. In *TWO-ROOM*, sampling uniformly from the transformed space corresponds to choosing more samples along the wall.

We ran DKBRL on *TWO-ROOM* with a large bandwidth ($b = .06$) to see if it could identify the wall. The results were successful; DKBRL was able to learn a metric that separated states on opposite sides of the wall. To visualize the metric, we sampled some points in the state space, calculated all-pairs-shortest-paths, and performed multidimensional scaling [14] to get a 2D projection. Figure 4.2 shows the projection resulting from the metric for one action; the projections for the other actions were similar.

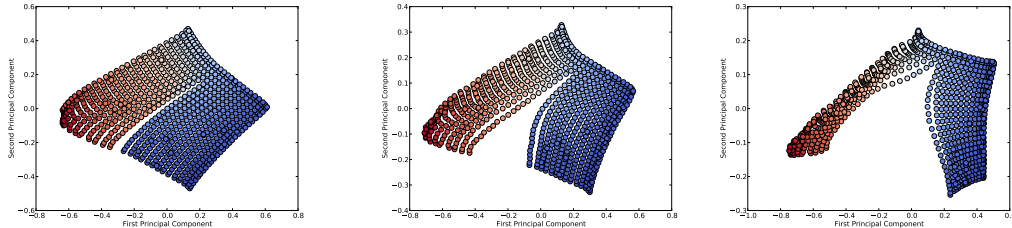


Figure 3: DKBRL opening the wall in *TWO-ROOM* over three iterations. Points are colored by ground truth value (red=high, blue=low). After the first iteration (left) a rift has started to form, by the third iteration points are completely separated by value.

5 Results

We start by demonstrating our approach work on Mountain-Car, a simple reinforcement learning domain that allows us to easily visualize the value function and gain insight about how DKBRL works. We then present our main results: performance improvements on the more challenging Acrobot and PinBall domains.

5.1 Mountain-Car (proof-of-concept)

Mountain-Car is a two dimensional MDP [6] modelling a car with a weak motor attempting to drive out of a valley.⁸ The car is not powerful enough to escape directly and must build up energy by rolling back and forth. Mountain-Car’s value function has a discontinuity that goes in a spiral

⁸ The code for Mountain-Car and Acrobot used for this paper was adapted from RL-Glue [15].

through the state space, separating states where the car has enough energy to make it up the hill on its current roll from states that require an additional back and forth.

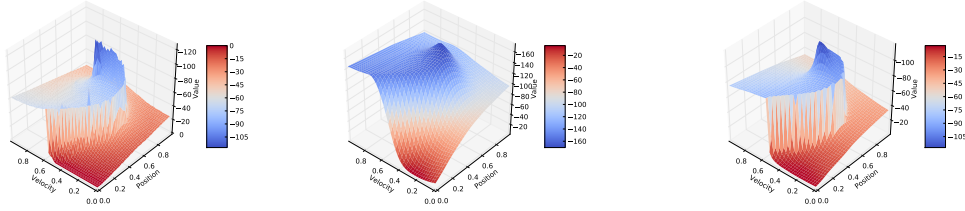


Figure 4: (Left to right) Mountain-Car’s value function; the value function as approximated by KBRL with d_{EUC} and $b = .09$; and the approximation after four iterations of DKBRL with $\alpha = 1$.

Our representation discovery algorithm allows KBRL to capture the discontinuity remarkably well. It is also able to find the correct value for the bottom of the hill (note the axes). Nonetheless, because Mountain-Car is such an easy problem, there is little difference in the policies induced by KBRL’s and DKBRL’s value function approximations. What matters for solution quality is not the value function approximation error, but that the best action gets assigned the highest Q-Value.

5.2 Acrobot

Acrobot is a four-dimensional MDP [6] modelling a two-link robot resembling a gymnast on a high bar. The gymnast can actuate at the waist and must raise its feet above some height by swinging back and forth. The acrobot domain has a value function discontinuity that resembles that of Mountain-Car.

For our experiments, we collected 15000 sample transitions per action, with start points selected to uniformly cover the reachable state space. We generated a solution from the transitions using KBRL then performed two iterations of DKBRL. We conducted three sets of experiments, one for each bandwidth: .03, .06, and .09. To account for the effects of random sampling we repeated each experiment 6 times and averaged the results. For each run, we chose $\alpha = .5$ because that worked well in our regression experiments in the supplementary materials.

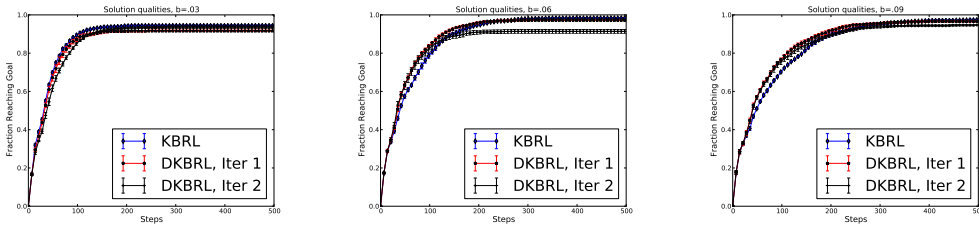


Figure 5: (Top to bottom) The average solution qualities for the three experiments. The plots show the cumulative distributions of steps-to-goal. The standard errors are drawn on the graph.

Figure 5 shows the average solution qualities for the three sets of experiments. Each plot shows cumulative distribution of the number of steps it took to reach the goal state from 230 start states selected to uniformly cover the reachable state space. Note that the plots are the averages of the 6 experiments performed at each bandwidth and that the standard-errors are drawn on the graph but are hard to see because they are so small.

We now point out the salient features of the graphs. In roughly 30% of states, the agent is near the end of a trajectory that reaches the goal (i.e. < 50 steps from the goal). In these easy states all the solutions perform the same. The solution quality in the remaining 70% of states is what matters.

For the size of our dataset, $b = .03$ is too small; KBRL undersmooths and produces a bad initial policy that doesn’t reach the goal for 5% of states. Performing DAWIT starting from this solution

amplifies the noise and produces even worse policies. When we chose the more reasonable $b = .06$, KBRL produces a good policy. One round of DKBRL is able to improve on this, slightly shortening the steps-to-goal for 65% of all states. The next round of DKBRL, however, is counter-productive, failing to reach the goal from 10% of states. When $b = .09$ the effects of oversmoothing the discontinuities starts to show for KBRL. The graph is much slower to rise than when $b = .06$. A round of DKBRL offers a sizeable improvement for 60% of states. The second round of DKBRL offers no additional improvement.

Since DAWIT is designed to solve the problem of oversmoothing at discontinuities, we would expect DKBRL to improve over KBRL when the bandwidth is large. This is what appears to be happening here, but it is difficult to say for sure because the graphs are so similar. Because the discontinuity in Acrobot’s value function is not along a decision boundary, improving the fit there does not do much for solution quality. In the next subsection, we consider a domain where discontinuities correspond to decision boundaries.

5.3 PinBall

PinBall is a four-dimensional MDP that models a ball navigating through a maze towards a goal [16]. The ball is dynamic, and bounces off obstacles; the five actions allow the ball to either stay in place or accelerate slightly along one of the compass directions. PinBall is particularly challenging because it is easy to get stuck on a wall while rounding a corner. Furthermore, some of the obstacles are so thin that they are hard to detect from the sample transitions.

We conducted our tests on one of the maps that came with the open source code.⁹ We had to make two modifications to the domain: first, we fixed a bug that allowed the ball to pass through walls under some circumstances and second, we increased the time discretization threefold so as to reduce the amount of data needed to solve the problem.

For this set of experiments, we collected 20000 sample transitions per action uniformly from the reachable state space. We then passed the samples through KBRL followed by two iterations of DKBRL. We did this four times each at bandwidths .04, .07 and .09 keeping the relaxation rate fixed at $\alpha = .5$. The resulting steps-to-goal cumulative distributions are shown in Figure 6.

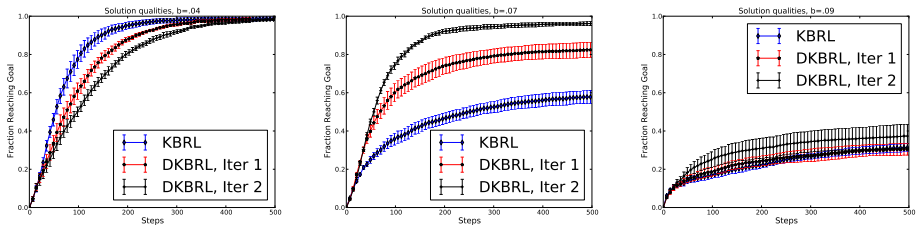


Figure 6: The average solution qualities for PinBall for $b = .04$, $.07$, and $.09$ respectively.

For our chosen sample size, $b = .04$ is near the optimal value for KBRL. KBRL produces its best solution there and performing iterations of DKBRL makes the performance worse. We suspect that this happens because the value function approximation produced by KBRL has large ripples¹⁰ which then get amplified by DAWIT making the fit worse.

When we raise the bandwidth to $b = .07$, the effects of oversmoothing kick in and the performance of KBRL plummets. Here DKBRL is able to counteract the bias resulting from oversmoothing and produce a solution comparable to the one produced by KBRL at $b = .04$. The resulting average for the second iteration of DKBRL with $b = .07$ is similar to that of KBRL with $b = .04$, but the variance is smaller.

Finally, when we raise the bandwidth to $.09$, the oversmoothing of KBRL is too much for DAWIT to undo. DKBRL manages to improve upon the initial solution, but not by much.

⁹ The code is available at <http://www-all.cs.umass.edu/~gdk/pinball/>. We used the map *pinball-easy.cfg*

¹⁰In our discussion of *TWO-ROOM* we note that performing KBRL with small bandwidths produces value functions with the right overall shape but with ripples

These experiments suggest that the key merit of DKBRL is that it can reduce the need for bandwidth tuning by allowing for near optimal solutions to be found over a wider interval of bandwidths.

6 Related Work

The method closest to ours for non-parametric regression is Metric Learning for Kernel Regression (MLKR) [17], which finds the Mahalanobis metric best suited for performing kernel regression. Using Mahalanobis distance is equivalent to applying a linear transform to the input space. Linear transforms are not powerful enough to smooth out discontinuities and would offer little help approximating *TWO-ROOM*'s value function. Predictive Projections [18] uses an approach similar to MLKR for dimensionality reduction in parametric reinforcement learning.

Other related algorithms are ST-ISOMAP [19] and Action Respecting Embedding [20], which use modified nearest-neighbors algorithms to discover and unroll the manifold containing the data. These algorithms have not been applied to RL. They would be well suited for learning a representation for problems where value function discontinuity arises from local state space topology.

Existing representation discovery algorithms for parametric RL have largely focused on modifying the parametric representation of the value function itself. One early approach was Proto-value functions (or PVFs) [10], which uses nearest neighbors on the sample transitions to discover the manifold of the state space and uses the eigenfunctions of the graph Laplacian as a basis for representing the value function. PVFs, along with the related diffusion wavelet approach [21], focus on the topology on the state space and offer little additional leverage when discontinuities arise from the MDPs reward structure. Another parametric approach is the use of Bellman-error basis functions (BEBF) [22], which are learned basis functions that represent the Bellman error in previous approximations. BEBFs are similar in spirit to the technique we present in this paper; however, they are used as basis functions in a linear value function approximation architecture.

We do not attempt to produce experimental results comparing our algorithm to any of the techniques presented above. They attempt to address problems that are related to, but distinct from, what DAWIT is designed for and there is no meaningful comparison that can be made.

7 Conclusion and Future Work

Representation discovery, which has so far been investigated primarily in parametric approaches to reinforcement learning, is a promising area in the context of nonparametric approaches. A particularly interesting next step would be to explore an online version of DKBRL to that samples new points for coverage in the transformed space. The correctness guarantees of KBRL require sampling points uniformly from the domain. Sampling uniformly from our transformed domain is equivalent to concentrating samples near value function discontinuities in the state space, which is desirable since that is where the value function is hardest to represent.

Acknowledgments

We would like to acknowledge the help of Leslie Kaelbling and Tomás Lozano-Pérez through every step of this project. We would also like to thank Tommi Jaakkola for a conversation about kernels.

References

- [1] Dirk Ormoneit and Šaunak Sen. Kernel-based reinforcement learning. *Machine learning*, 49(2-3):161–178, 2002.
- [2] Dirk Ormoneit and Peter Glynn. Kernel-based reinforcement learning in average-cost problems. *IEEE Transactions on Automatic Control*, 47(10):1624–1636, 2002.
- [3] André da Motta Salles Barreto, Doina Precup, and Joelle Pineau. Reinforcement learning using kernel-based stochastic factorization. In *Advances in Neural Information Processing Systems 24*, pages 720–728, 2011.
- [4] André da Motta Salles Barreto, Doina Precup, and Joelle Pineau. On-line reinforcement learning using incremental kernel-based stochastic factorization. In *Advances in Neural Information Processing Systems 25*, pages 1493–1501, 2012.

- [5] André MS Barreto, Doina Precup, and Joelle Pineau. Practical kernel-based reinforcement learning. Technical report, Laboratrio Nacional de Computao Cientfica, May 2014.
- [6] Richard S Sutton and Andrew G Barto. *Reinforcement learning: An introduction*. MIT press, 1998.
- [7] Martin L Puterman. *Markov Decision Processes: Discrete Stochastic Dynamic Programming*, volume 414. John Wiley & Sons, 2009.
- [8] Justin A Boyan. Least-squares temporal difference learning. In *Proceedings of the 16th International Conference on Machine Learning*, pages 49–56, 1999.
- [9] Gavin A Rummery and Mahesan Niranjan. *On-line Q-learning using connectionist systems*. University of Cambridge, Department of Engineering, 1994.
- [10] Sridhar Mahadevan and Mauro Maggioni. Proto-value functions: A Laplacian framework for learning representation and control in Markov decision processes. *Journal of Machine Learning Research*, 8(10), 2007.
- [11] Jacqueline K Benedetti. On the nonparametric estimation of regression functions. *Journal of the Royal Statistical Society*, pages 39:248–253, 1977.
- [12] Dawit Zewdie. Representation discovery in non-parametric reinforcement learning. Master’s thesis, MIT, Cambridge MA, 2014.
- [13] Lihong Li, Thomas J Walsh, and Michael L Littman. Towards a unified theory of state abstraction for MDPs. In *International Symposium on Artificial Intelligence and Mathematics*, 2006.
- [14] Joseph B Kruskal. Multidimensional scaling by optimizing goodness of fit to a nonmetric hypothesis. *Psychometrika*, 29(1):1–27, 1964.
- [15] Brian Tanner and Adam White. RL-Glue : Language-independent software for reinforcement-learning experiments. *Journal of Machine Learning Research*, 10:2133–2136, September 2009.
- [16] George Konidaris and Andrew G Barto. Skill discovery in continuous reinforcement learning domains using skill chaining. In *Advances in Neural Information Processing Systems 22*, pages 1015–1023, 2009.
- [17] Kilian Q. Weinberger and Gerald Tesauro. Metric learning for kernel regression. In *11th International Conference on Artificial Intelligence and Statistics*, 2007.
- [18] Nathan Sprague. Predictive projections. In *International Joint Conference on Artificial Intelligence*, pages 1223–1229, 2009.
- [19] Odest Chadwicke Jenkins and Maja J Matarić. A spatio-temporal extension to ISOMAP nonlinear dimension reduction. In *Proceedings of the 21st International Conference on Machine Learning*, page 56, 2004.
- [20] Michael Bowling, Ali Ghodsi, and Dana Wilkinson. Action respecting embedding. In *Proceedings of the 22nd International Conference on Machine Learning*, pages 65–72. ACM, 2005.
- [21] Sridhar Mahadevan and Mauro Maggioni. Value function approximation with diffusion wavelets and Laplacian eigenfunctions. In *Advances in Neural Information Processing Systems 18*, pages 843–850, 2006.
- [22] Ronald Parr, Christopher Painter-Wakefield, Lihong Li, and Michael Littman. Analyzing feature generation for value-function approximation. In *Proceedings of the 24th International Conference on Machine Learning*, pages 737–744. ACM, 2007.

A Transforming For Improved Fit

This section provides a different interpretation of DAWIT, the metric learning algorithm presented in Section 4.1. We start by introducing Fit-Improving Iterative Representation Adjustment (FIIRA), a function approximation framework under which DAWIT falls. We then present an intuitive explanation of the rationale behind DAWIT.

A.1 Fit-Improving Iterative Representation Adjustment

The problem statement of curve-fitting is as follows: given a set of training points, $D = \{(x_i, y_i) \mid i = 1, \dots, n\}$, of point-value pairs with $y_i = f(x_i)$ for some function $f : X \rightarrow \mathbb{R}$, produce a function \tilde{f} to approximate f well, for some measure of approximation quality.

A regressor, r , is a procedure for creating fits from some space of functions, \mathcal{F}_r . If f is not well approximated by any function in \mathcal{F}_r , the fit generated by r is guaranteed to be poor. One way to fix this problem is to transform the domain of f and work in a space where f is well approximated. Choosing such a transform requires prior knowledge or assumptions about f .

Since we are not in a position to make assumptions about f , we wish to infer a transform directly from the data. Our idea for doing so, is to pass D to the regressor, then use the approximation produced to infer a transform Φ of the domain X such that f on $\Phi(X)$ is better approximated by \mathcal{F}_r . Algorithm 1 describes the framework for doing this. The procedure takes as input a dataset, D ; a regressor, $REGR$; and a transform generator, TF .

Algorithm 2 Fit-Improving Iterative Representation Adjustment

```

1: procedure FIIRA( $D, REGR, TF$ )
2:    $\Phi_0 \leftarrow x \mapsto x$  ▷ Identity transform
3:    $D_0 \leftarrow D$ 
4:    $i \leftarrow 0$ 
5:   repeat
6:      $\tilde{f}_{i+1} \leftarrow REGR(D_i)$  ▷ Perform regression
7:      $\Phi_{i+1} \leftarrow TF(\tilde{f}_{i+1}, D_i)$  ▷ Produce transform
8:      $D_{i+1} \leftarrow \{(\Phi_{i+1}(x), y) \mid (x, y) \in D_i\}$  ▷ Update the dataset
9:      $i \leftarrow i + 1$ 
10:  until  $\tilde{f}_i \approx \tilde{f}_{i-1}$  ▷ Or until best fit attained
11:  return  $x \mapsto \tilde{f}_i(\Phi_{i-1}(x))$ 
12: end procedure

```

A formal analysis of the properties of FIIRA for a general regression scheme and transform generator is outside the scope of this paper and is left for future work. What follows is a discussion of FIIRA for the special case where the regressor is a local-averaging kernel smoother and the transform generator is DAWIT.

A.2 Dimension-Adding Wrinkle-Ironing Transform

In the paper we claim that the metric created by DAWIT corresponds to a transform that warps the state space through a higher dimension. We now elaborate on that.

Consider a transform generator that, given a function f with domain X , returns a transform Φ which maps every $x \in X$ to $\langle x \mid f(x) \rangle$ (the bar represents concatenation). Φ stretches X into $d + 1$ dimensions in a way that pulls apart points that differ in value (See Figure 6).

After the transformation, the distance between two points a and b in the domain of f becomes

$$\|\Phi(a) - \Phi(b)\| = \sqrt{\|a - b\|^2 + (f(a) - f(b))^2}.$$

Note that $\|\Phi(a) - \Phi(b)\|$ varies more closely with $|f(a) - f(b)|$ than does $\|a - b\|$.

The transform Φ does what we want, but it has two problems; it is sensitive to the scale of f , and it can change the diameter of X . We fix these problems by normalizing f by $\alpha\mu_f$ and $\Phi(X)$ by c_0 (as defined in the main body of the paper).

With these two changes, Φ maps the m -dimensional vector, $x = (x_1, \dots, x_m)$ to the $m + 1$ -dimensional $x' = (c_0x_1, \dots, c_0x_m, c_0\alpha\mu_f \cdot f(x))$. The distance metric that corresponds to the final form of this transform is

$$\|\Phi(a) - \Phi(b)\| = c_0 \sqrt{\|a - b\|^2 + \alpha^2 \mu_f^2 \cdot (f(a) - f(b))^2}.$$

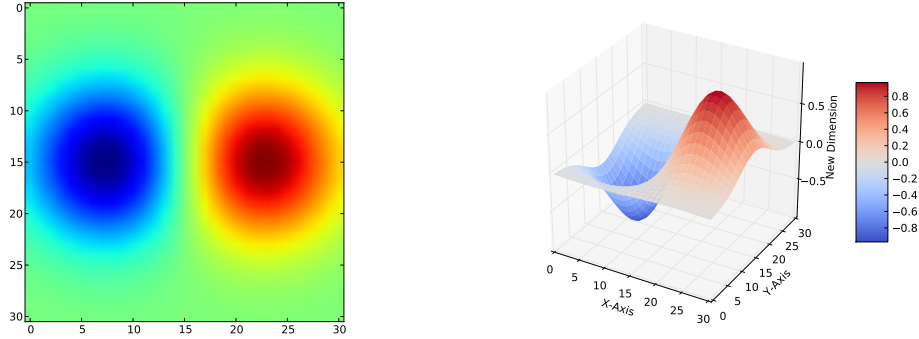


Figure 7: The figure on the left is a heatmap of some function with a two-dimensional domain. The areas in red are where it attains a high value and the ones in blue are where it attains a low value. The figure on the right shows the two-dimensional domain stretched through three dimensional space in such a way that separates points that differ in value. The red areas are pulled up and out of the page while the blue ones are pushed down and into the page. Distances in this transformed space correspond to the metric produced by DAWIT.

When we substitute for μ_f and c_0 , this equals the metric produced by DAWIT; hence the name “dimension-adding” VCPM relaxation. We refer to kernel regression augmented to use DAWIT as FDK because it is a FIIRA approach combining DAWIT and Kernel-regression.

A.3 How DAWIT works

Kernel-regression produces function estimates using local averaging. As a result, the approximation is good where the target function, f , is linear and bad where it has high curvature. It follows that the curvature of the estimate, $h(x)$, is correlated with the approximation error. Thus, we can infer where the approximation likely to be poor just by looking at the approximation.

We use this insight to construct a transform of the input domain, X , into a space where h (and thus also f) are smoother. Our transform warps the m dimensional X into the $m + 1$ dimensional X' in such a way that its diameter is preserved but some neighborhoods grow or shrink depending on the slope of h . The metric produced by DAWIT corresponds to distances in X' .

Let f be the unit step function and let $X = [-1, 1]$. One iteration of kernel regression produces h resembling a sigmoid. h attains its maximum slope near $x = 0$. Performing DAWIT with h produces a metric, d , that stretches the area around $x = 0$ (i.e. $d(-\epsilon, \epsilon) > 2 * \epsilon$, for small $|\epsilon|$) and squashes the regions near $x = 1$ and $x = -1$. The point $x = 0$ itself may get moved closer to $x = 1$ or $x = -1$, but that does not matter. What matters is that on the next round of regression the region around $x = 0$ is magnified, making it easier to pinpoint where the discontinuity lies. This magnification is analogous to using a smaller bandwidth at $x = 0$.

One can see now why we call the transform “wrinkle-ironing”. The discontinuity in the step function resembles a crease on an article of clothing. Repeated application of the transform smooths this and similar value cliffs much like a hot iron passing over a wrinkly shirt.

A.4 Value Consistent Pseudometric

In the main body of the paper, we claimed that using the VCPM as a valid metric in kernel regression was theoretically sound. We now justify that claim.

When viewed under the lens of a FIIRA approach, the VCPM can be seen as coming from a transform Φ^* that satisfies $\|\Phi^*(x) - \Phi^*(x')\| = \mu_f |f(x) - f(x')|$. A transform that satisfies this property is $\Phi^*(x) = \mu_f f(x)$. Under this interpretation, we are mapping each point to its scaled value and performing kernel regression to fit a line. Only points with identical values get mapped to the same point by the transform. Since Φ^* is a safe to use before doing regression, performing kernel regression with the VCPM for the function being approximated cannot cause problems.

B Graphs

This section contains graphical demonstrations of the convergence properties of FDK. It starts by showing how FDK converges to a piecewise flat approximation when modelling a line. It goes on to show the FDK fits generated for some datasets.

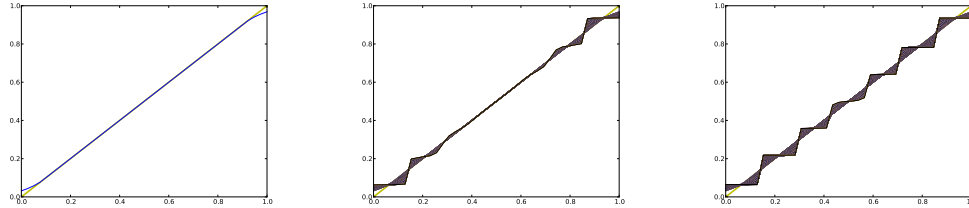


Figure 8: How FDK converges to a piecewise flat approximation when attempting to fit a line. The figure on the left shows the first fit f_0 in blue. Note how the fit is biased at the boundaries. This bias gets amplified over the next several iterations of FDK (middle). The end result is the piecewise flat approximation on the right. If we had used a smaller bandwidth there would have been more pieces in the piecewise flat approximation.

When fitting a line, the approximation error increases with every iteration. For most functions, however, the error goes down for a few iterations before going up. The following figures show the result fitting some select functions with different combinations of parameters.

Below we have included plots that show approximation quality of FDK for some select datasets. The plots on the left show the dataset (scatter plot), the kernel regression fit (dotted blue line), the best FDK fit obtained (solid red line), and the piecewise flat function to which FDK converges for the value of α that produced the best fit (green pluses). The plots on the right show how the approximation error changes as a function of iteration number for different values of α . Approximation error is measured as the sum of squared errors, normalized so that the fit produced by the vanilla kernel regression has unit error. Note how low the error dips and how few iterations it takes to get there.

